Structural Basis for a Change in Substrate Specificity: Crystal Structure of S113E Isocitrate Dehydrogenase in a Complex with Isopropylmalate, Mg^{2+}, and NADP[†,‡]

Sharon A. Doyle,[§] Peter T. Beernink,[||] and Daniel E. Koshland, Jr.*[,§]

Department of Molecular and Cell Biology, University of California at Berkeley, Berkeley, California 94720, and Molecular and Structural Biology Division, Lawrence Livermore National Laboratory, 7000 East Avenue, L-448, Livermore, California 94550

Received November 3, 2000; Revised Manuscript Received January 30, 2001

ABSTRACT: Isocitrate dehydrogenase (IDH) catalyzes the oxidative decarboxylation of isocitrate and has negligible activity toward other (*R*)-malate-type substrates. The S113E mutant of IDH significantly improves its ability to utilize isopropylmalate as a substrate and switches the substrate specificity (k_{cat}/K_M) from isocitrate to isopropylmalate. To understand the structural basis for this switch in substrate specificity, we have determined the crystal structure of IDH S113E in a complex with isopropylmalate, NADP, and Mg^{2+} to 2.0 Å resolution. On the basis of a comparison with previously determined structures, we identify distinct changes caused by the amino acid substitution and by the binding of substrates. The S113E complex exhibits alterations in global and active site conformations compared with other IDH structures that include loop and helix conformational changes near the active site. In addition, the angle of the hinge that relates the two domains was altered in this structure, which suggests that the S113E substitution and the binding of substrates act together to promote catalysis of isopropylmalate. Ligand binding results in reorientation of the active site helix that contains residues 113 through 116. E113 exhibits new interactions, including van der Waals contacts with the isopropyl group of isopropylmalate and a hydrogen bond with N115, which in turn forms a hydrogen bond with NADP. In addition, the loop and helix regions that bind NADP are altered, as is the loop that connects the NADP binding region to the active site helix, changing the relationship between substrates and enzyme. In combination, these interactions appear to provide the basis for the switch in substrate specificity.

Understanding how enzymes discriminate between ligands such as substrates and inhibitors is crucial for the development of rationally designed drugs. The advent of random mutagenesis methods such as DNA shuffling (*1*, *2*) has increased the number of successful attempts of protein engineering by identifying amino acid substitutions that have unpredictable structural effects and therefore would have been difficult to design rationally. However, in many cases an understanding of how substitutions exert their effects remains elusive. Therefore, it is valuable to assess the effects of randomly generated beneficial substitutions on protein structure at the atomic level.

The isocitrate dehydrogenase (IDH)[1] of *Escherichia coli* [*threo*-DS-isocitrate:$NADP^+$ oxidoreductase (decarboxylating), EC 1.1.1.42] catalyzes the conversion of the substrates isocitrate and NADP to the products α-ketoglutarate, NADPH, and CO_2 in the presence of Mg^{2+}. Many X-ray crystallographic and enzyme kinetic studies have identified important structural and catalytic features that contribute to IDH activity (*3*−*7*). The γ-carboxylate group of isocitrate forms a hydrogen bond to S113 in the active site and a salt bridge with the charged nitrogen of the nicotinamide ring of NADP (*6*). These interactions stabilize the substrates in the active site and align the substrates and catalytic residues for efficient catalysis. IDH exhibits dramatically reduced activities toward malate derivatives that lack the γ-carboxylate (*5*).

Previously, attempts were made to engineer IDH to utilize substrates similar to isocitrate that lacked the charged γ-carboxylate group (*5*). Residue S113 in the active site of IDH was replaced by an acidic residue in order to mimic the γ-carboxylate of the natural substrate, isocitrate, when alternative substrates were used. However, neither S113D nor S113E mimicked the role of the isocitrate γ-carboxylate in stabilizing the binding of NADP, as judged by the Michaelis constant (K_M) of NADP using malate as the substrate. In addition, whereas S113E showed small improvements in apparent affinity (K_M, ∼3-fold) and turnover number (k_{cat}, ∼2-fold) of other malate-derived alternative substrates with uncharged γ moieties, the effects were generally reduced as the size of the γ substituent increased.

Inconsistent with this pattern, however, was the recent finding that the S113E mutation identified in a random mutagenesis experiment changed the substrate specificity of

[†] Support was obtained from NSF Grant MCB 9723372 to D.E.K. and NIH Postdoctoral Fellowship GM 19582 to S.A.D.

[‡] The atomic coordinates and structure factor amplitudes have been deposited in the Protein Data Bank, accession number 1HJ6.

* Corresponding author. Telephone: 510-642-0416. Facsimile: 510-643-6386. E-mail: DEK@uclink4.berkeley.edu.

[§] University of California at Berkeley.

[||] Lawrence Livermore National Laboratory.

[1] Abbreviations: IDH, isocitrate dehydrogenase; IPMDH, isopropylmalate dehydrogenase; NAD, β-nicotinamide adenine dinucleotide; NADP, β-nicotinamide adenine dinucleotide phosphate; NADPH, reduced β-nicotinamide adenine dinucleotide phosphate.

10.1021/bi002533q CCC: $20.00
Published on Web 03/16/2001

Table 1: Kinetic Constants of IDH and IPMDH Enzymes toward Isopropylmalate and Isocitrate

		IDH[a]	IDH^{S113E} [a]	IPMDH[b]
IPM	k_{cat} (s^{-1})	3.4×10^{-4}	5.5×10^{-4}	1.9×10^{1}
	K_M (μM)	200	5	44
	k_{cat}/K_M	1.7×10^{-6}	1.0×10^{-4}	4.3×10^{-1}
ISO	k_{cat} (s^{-1})	8.0×10^{1}	6.1×10^{-2}	
	K_M (μM)	5	1190	
	k_{cat}/K_M	1.6×10^{1}	5.1×10^{-5}	

[a] Kinetic values toward isopropylmalate (IPM) and isocitrate (ISO) for IDH enzymes were taken from Doyle et al. (*8*). [b] IPMDH values were obtained from Wallon et al. (*30*).[2]

IDH away from isocitrate toward isopropylmalate (*8*), which is larger and bulkier than all of the alternative substrates used in previous studies. This single mutation improved the apparent affinity of isopropylmalate 37-fold and the turnover number 1.6-fold compared to wild-type IDH, resulting in an overall improvement in catalytic efficiency (k_{cat}/K_M) of 59-fold (Table 1).

In this work, we sought to determine how the S113E substitution affected the structure of IDH in the presence of isopropylmalate, Mg^{2+}, and NADP to provide insight into its improved activity toward this nonphysiological substrate. Specifically, we were interested in how the presence and conformation of residue E113 affected the other active site residues and substrates. In addition, we wondered if the S113E substitution caused more global changes in structure or flexibility of the enzyme. Here we report the X-ray crystal structure of IDH S113E in an active complex with isopropylmalate, Mg^{2+}, and NADP obtained by cryocrystallographic trapping methods.

METHODS

Protein Purification and Crystallization Procedures. S113E IDH was expressed from the plasmid pTK513 in an *E. coli* strain JLK-1, which has the IDH gene deleted. IDH purification was performed as previously described (*9*). IDH concentrations were determined at 280 nm using a molar extinction coefficient of 66 300 M^{-1} cm^{-1} (*10*). The IDH protein was stored in final buffer (5 mM Na_2HPO_4, 100 mM NaCl, and 5% glycerol, pH 6.0) at −80 °C.

Purified IDH protein was diluted 2-fold with 2× crystallization buffer (70 mM Na_2HPO_4, 18 mM citric acid, 200 mM NaCl, and 0.4 mM DTT, pH 5.4) and concentrated to 25, 30, 35, and 40 mg/mL using a Millipore Ultra free-MC filter unit. IDH crystals (0.2 × 0.2 × 0.2 mm) were obtained by vapor diffusion at 4 °C from hanging drops containing 5 μL each of 34−44% $(NH_4)_2SO_4$ solutions in 1× crystallization buffer (35mM Na_2HPO_4, 9 mM citric acid, 100 mM NaCl, and 0.2 mM DTT, pH 5.4) and 5 μL of purified protein. The crystals grew in space group $P4_32_12$ with unit cell dimensions $a = 105.38$, $b = 105.38$, and $c = 146.48$ Å and one subunit of the IDH dimer in the asymmetric unit. Crystals that were first equilibrated into a soaking solution containing 50% saturated $(NH_4)_2SO_4$, 30% glycerol, and 25 mM Tris·HCl, supplemented with substrates, 200 mM D,L-*threo*-3-isopropylmalic acid (WAKO Bioproducts, Richmond, VA), 200 mM NADP, and 100 mM $MgCl_2$, pH 7.8 ("1×"), cracked immediately. Consequently, substrate soaks were carried out in a series of four conditions with increasing concentrations of glycerol and substrates, for approximately 15−30 min each: (1) 0.5% glycerol, no substrates; (2) 5% glycerol, 0.1× substrates; (3) 15% glycerol, 0.5× substrates; (4) 30% glycerol, 1× substrates. Intact crystals recovered from the last soak were flash cooled on a nylon loop and stored in liquid N_2.

Structure Determination. Data were collected from a single crystal at 100 K using an ADSC Quantum 4 CCD detector at beam line 5.0.2, Advanced Light Source, Lawrence Berkeley National Laboratory. The data were integrated using MOSFLM (*11*) and scaled with SCALA (*12*) to give $R_{sym} = 0.088$ for 56 218 independent reflections from 21.2 to 2.0 Å resolution. The data were 98.8% complete overall (100.0% in the 2.11−2.00 Å resolution shell), with an $I/\sigma I$ value of 9.3 overall (2.5 in the outer shell). The structure was solved by molecular substitution using a model derived from the structure of wild-type IDH in complex with isopropylmalate, Mg^{2+}, and NADP, "IPM·IDH" (A. Mesecar and D. E. Koshland, Jr., unpublished results), from which the ligands and solvent had been removed. Rigid body, positional and restrained *B* factor refinement were carried out with X-PLOR (*13*) using data from 6.0 to 2.0 Å resolution with $F > 2.0\sigma$. Ligands were added manually with O (*14*), and automated solvent building used ARP/wARP (*15*). Iterative cycles of refinement and manual rebuilding in O were performed until the R_{free} converged. Validation of the model was carried out with PROCHECK (*12*) and WHATCHECK (*16*).

Structure Analysis. Superpositions were performed using the program GEM *(17)* based on residues that bind the conserved malate-binding core of the substrates (residues 119, 129, 230, 283, 307, 311). Hinge angle differences were calculated as the angle of rotation required to reorient two molecules from superposition of domain 1 (residues 1−119, and 325−416) to superposition of domain 2 (residues 121−317). Domain 1 backbone atoms chosen for the hinge analysis exhibited <1.2 Å root-mean-square (rms) deviation when domain 1 was superimposed. Domain 2 was superimposed using the conserved malate-binding residues (residues 119, 129, 230, 283, 307, 311). Figures were generated with XtalView (*18*) and Raster3D (*19*) or InsightII (Molecular Simulations, Inc.).

RESULTS

Description of Structure. The crystal structure of IDH S113E in complex with isopropylmalate, Mg^{2+}, and NADP (IPM·IDH^{S113E}) was determined at 2.0 Å resolution by molecular substitution (see Methods). The electron density for residues 3−416 was continuous and easily interpretable in $2F_o - F_c$ electron density maps (Figure 1A). The ligands isopropylmalate, NADP, and Mg^{2+} were clearly present in the active site, as seen in omit $F_o - F_c$ maps (Figure 1B). The electron density was clearly defined for the entire NADP molecule, including the nicotinamide ring and adjacent ribose, which are often not well defined in density of IDH structures (such as in the IDH·IPM and ISO·IDH^{Y160F} structures described below). The structure has been refined to *R* and R_{free} values of 0.206 and 0.246 (Table 2). The model includes residues 3−416 (3199 protein atoms), one isopropylmalate, one NADP, two glycerol, and 232 water molecules, and one Mg^{2+} ion. Eighty-six percent of residues are in the most favored regions of a Ramachandran plot. The rms deviations from ideal bond lengths and angles were 0.006 Å and 1.20°, respectively.

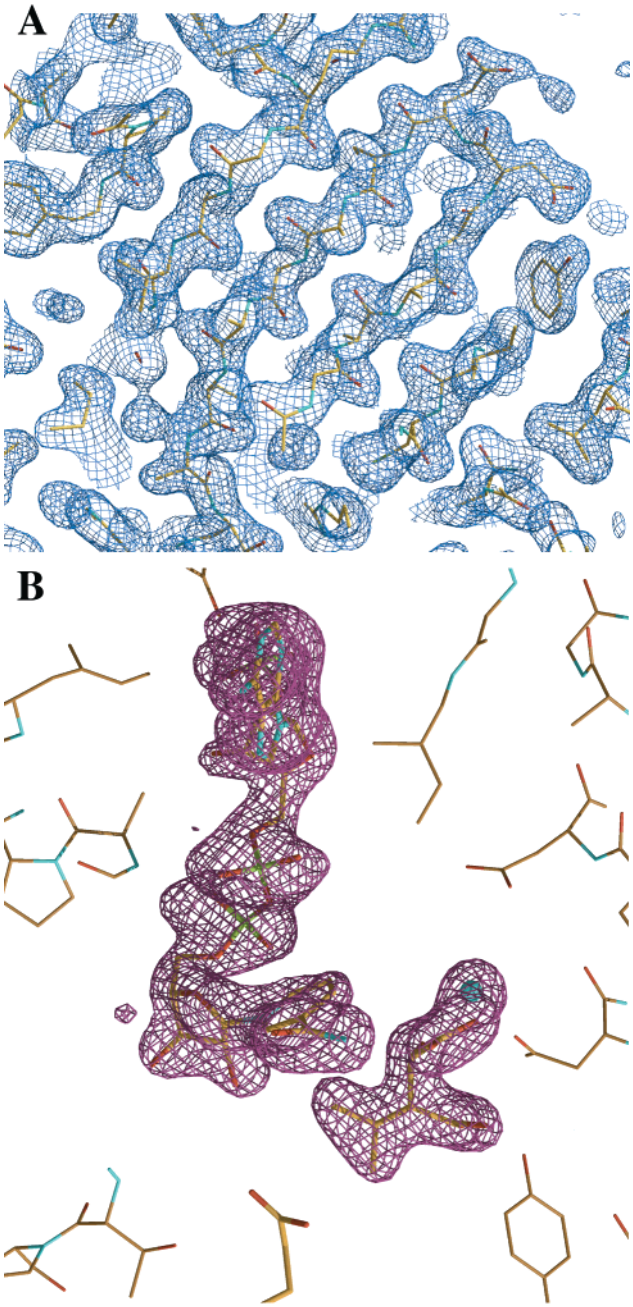

FIGURE 1: Electron density maps of IPM·IDH^{S113E}. (A) Representative $2F_o - F_c$ density map in a β-sheet region (contour level 1σ). (B) Omit $F_o - F_c$ map in the vicinity of the active site (contour level 4σ). NADP, isopropylmalate, and Mg^{2+} were omitted from the model, and sigma A weighted maps (*30*) were calculated as implemented in SIGMAA (*12*).

Structural Comparisons. Comparison of the structure of the S113E active complex to other IDH structures allows the identification of structural changes that occur due to the interactions of E113 with isopropylmalate and NADP. The structures were named using the substrate isocitrate (ISO) or isopropylmalate (IPM), if present (if so, NADP and Mg^{2+} were also present), followed by the enzyme, with amino acid substitutions in superscript. The newly determined structure of IDH containing the S113E mutation with isopropylmalate, Mg^{2+}, and NADP bound to the active site (IPM·IDH^{S113E}) was compared with the following three structures: (1) unliganded IDH containing the S113E mutation (IDH^{S113E}) (*20*) to assess changes in the mutant enzyme upon substrate binding; (2) a catalytically deficient mutant, Y160F, with bound isocitrate, Mg^{2+}, and NADP that was solved by time-resolved Laue crystallography (ISO·IDH^{Y160F}) (*3*) to understand the effects of the S113E substitution in the context of the bound substrates; and (3) wild-type IDH in complex with isopropylmalate, Mg^{2+}, and NADP (IPM·IDH) (A. Mesecar, D. E. Koshland, Jr., unpublished results) to see how the S113E substitution changes the interactions with isopropylmalate and NADP in the active site. Several regions of IPM·IDH ^{S113E} associated with the active site display structural changes upon binding substrates, shown in Figure 2. These include the interdomain hinge regions (residues 134−146 and 318−324), which affect the spatial relationship between the two domains of the IDH subunit, and several loops and a helix that contribute residues to the active site. No significant changes were seen in the relative orientation of subunits in the IDH dimer.

Table 2: Data Collection and Refinement Statistics

crystal	
space group	$P4_32_12$
cell dimensions (Å)	
a	105.38
b	105.38
c	146.48
data collection	
resolution range (Å)	21.2−2.0
unique/measured reflections	56218/265721
completeness (%)[a]	98.8 (100.0)
average $I/\sigma I$[a]	9.3 (2.5)
R_{sym}[a,b]	0.088 (0.709)
refinement	
R_{cryst}	0.206
R_{free}	0.246
RMS deviations	
bond lengths (Å)	0.006
bond angles (deg)	1.20

[a] Numbers in parentheses represent data in the highest resolution shell. [b] $R_{sym} = \sum_i(\sigma_j|I_{ij} - \langle I_i\rangle|)/\sigma_i\langle I_i\rangle$.

Interdomain Hinge Changes. Comparison of superpositions of domain 1 (residues 1−119, 325−416) and domain 2 (residues 121−317) of IPM·IDH^{S113E} and IDH^{S113E} shows a rigid body movement of one domain relative to the other. Since the N- and C-termini of IDH are both in domain 1, two loop regions comprising residues 134−146 and residues 318−324 (Figure 2) connect the two domains and together act as a hinge. The relative orientation of domains can be described by an interdomain hinge angle. Close inspection of the hinge regions in IPM·IDH^{S113E} reveals local conformational changes relative to the other structures that accompany the interdomain hinge differences (Table 3), including backbone shifts of residues 318−322 of up to 1.7 Å and a change in the orientation of residue 322. The largest differences were observed between IPM·IDH^{S113E} and the structure of the inactive complex IPM·IDH (3.6°) and IDH^{S113E} (3.0°). The interdomain hinge angle difference between IPM·IDH^{S113E} and the active complex ISO·IDH^{Y160F} was 2.8°. Much smaller pairwise differences were seen between IPM·IDH and IDH^{S113E} (0.9°), IPM·IDH and ISO·IDH^{Y160F} (1.2°), and IDH^{S113E} and ISO·IDH^{Y160F} (0.3°).

Secondary Structural Changes. (A) Loop Region 255−263. Structural differences in the loop region composed of residues 255−263, which forms a structural feature near the active site from the opposite subunit of the IDH dimer, can be seen in all the structures compared (Figure 2). The

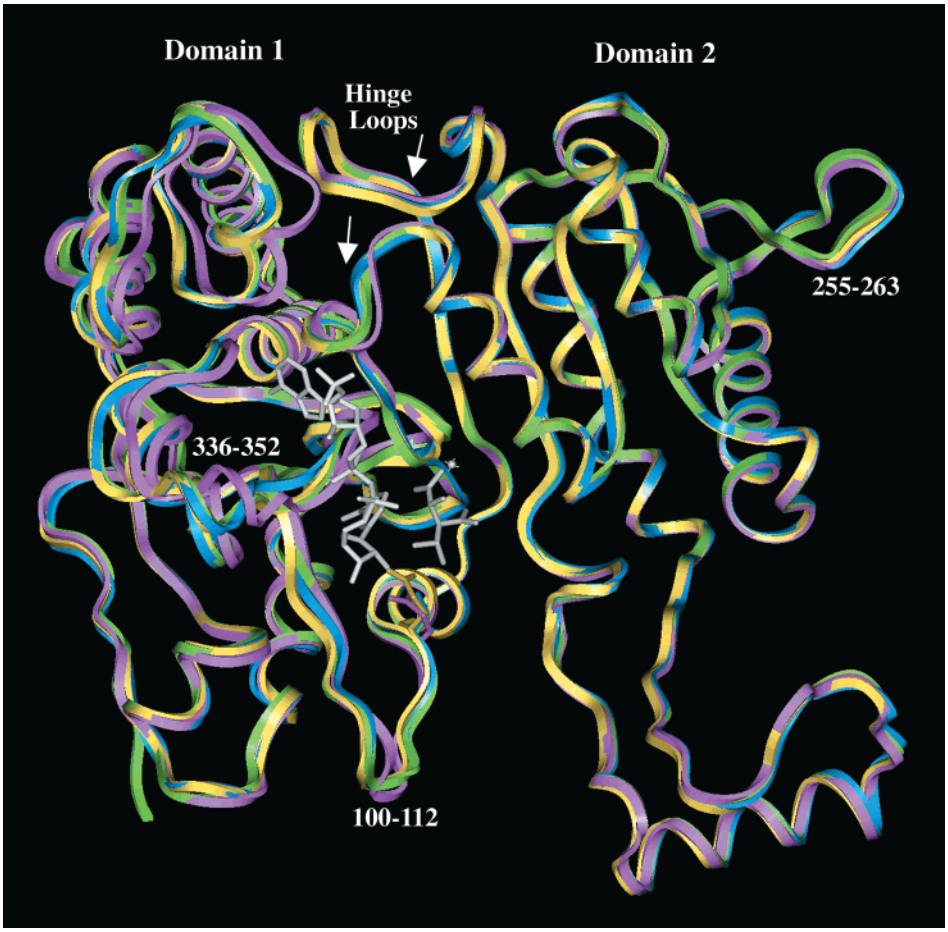

FIGURE 2: Superpositions of IDH structures show hinge differences and conformational rearrangements. IPM·IDH^{S113E} (pink), IDH^{S113E} (yellow), ISO·IDH^{Y160F} (blue), and IPM·IDH (green) are shown. Residue 113 is shown in stick rendering. Isopropylmalate, NADP, and Mg^{2+} of IDH^{S113E}ipm are also shown in stick rendering (white). Domains 1 and 2 of the IDH subunit are labeled, as are the hinge loops that connect the two domains (134−146 and 318−324). Regions exhibiting significant conformational changes include loop 100−112, loop 255−263, and loop 336−352 and are labeled accordingly.

Table 3: Interdomain Hinge Differences among IDH Structures

	IPM·IDH	ISO·IDH^{Y160F}	IDH^{S113E}
IPM·IDH^{S113E}	3.6° (3.97 Å)	2.8° (3.75 Å)	3.0° (4.12 Å)
ISO·IDH^{Y160F}	1.2° (0.88 Å)		0.3° (0.61 Å)
IDH^{S113E}	0.9° (0.55 Å)	0.3° (0.61 Å)	

differences in C-α positions ranged from 0.3 to 1.1 Å for all four structures, with IPM·IDH^{S113E} exhibiting an intermediate position relative to the other structures. D259 also displays reorientation of its side chain, with β and γ carbons 2.9−3.3 Å apart among the four structures. This contrasts with nearly all of the remainder of domain 2, which superimposes very closely in all four structures.

(B) NADP-Binding Loop (336−352) and Helix (390−397). Positional differences in backbone atoms were observed in the NADP-binding loop and helix regions, comprising loop residues 336−352 and helix residues 390−397, between IPM·IDH^{S113E} and all the other structures (Figures 2 and 3). These regions contain many residues identified in binding the adenine ring and 2′-phosphate of NADP as well as E336, contained in the binding loop, which is thought to interact with the carboxyamide nitrogen of the nicotinamide ring (*21*). Comparison of this loop in IPM·IDH^{S113E} and the unliganded structure shows backbone differences of up to 2.3 Å (residue 344 C-α), and similar movements are seen for the helix. These movements are independent from the interdomain hinge changes and are still evident when S113E is superimposed using domain 1, which includes these regions, to account for the change in interdomain hinge angle. The position of bound NADP changes in comparison to the other structures compared due to these structural alterations.

(C) Active Site Loop Alteration. The loop spanning residues 100−112 that connects the NADP-binding site to the active site helix shifts up toward the active site (Figures 2 and 4). Valine 107 shifts its position by 0.4−0.9 Å, significantly altering the positions of the following glycine residues (108−110) by 2.5−3.3 Å. This movement results in R112 being 1.6−1.8 Å farther toward the active site and interacting with E121 instead of E164, which may help to anchor the altered conformation of the loop and stabilize the tilted conformation of the active site helix, described below. Included in this loop movement is the repositioning of T104, which has been implicated in forming favorable interactions with the ribose moiety of NADP. This residue adopts a different position in all four structures compared (C-α differences of 0.6−1.8 Å) and is the farthest from the active site in the unliganded IDH^{S113E} structure, suggesting that interaction with the substrate or cofactor affects this residue by drawing it toward the active site.

(D) Active Site Helix Tilt. The N-terminal end of the active site helix of IPM·IDH^{S113E} is also shifted, tilting downward, away from the substrates as compared to IDH^{S113E} (Figures

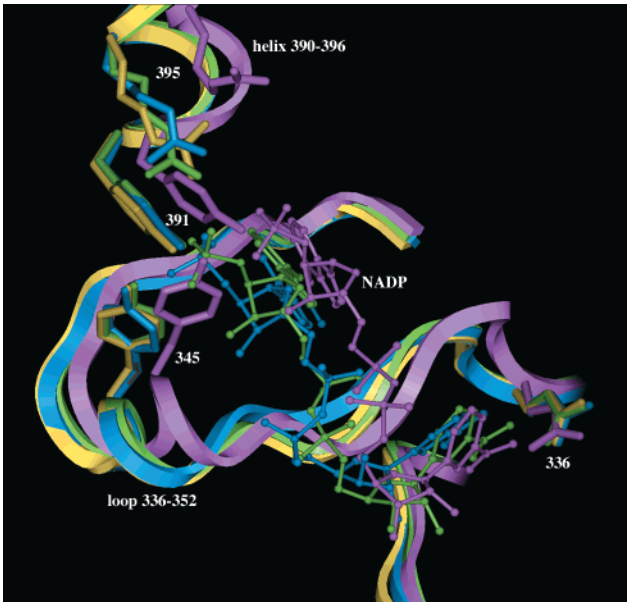

FIGURE 3: Superpositions showing the NADP binding loop and helix movement in IPM·IDH^{S113E} (pink) compared to IDH^{S113E} (yellow), ISO·IDH^{Y160F} (blue), and IPM·IDH (green). The loop and helix regions are shown as a ribbon, NADP is shown in ball-and-stick rendering, and some of the NADP binding residues are shown in stick rendering.

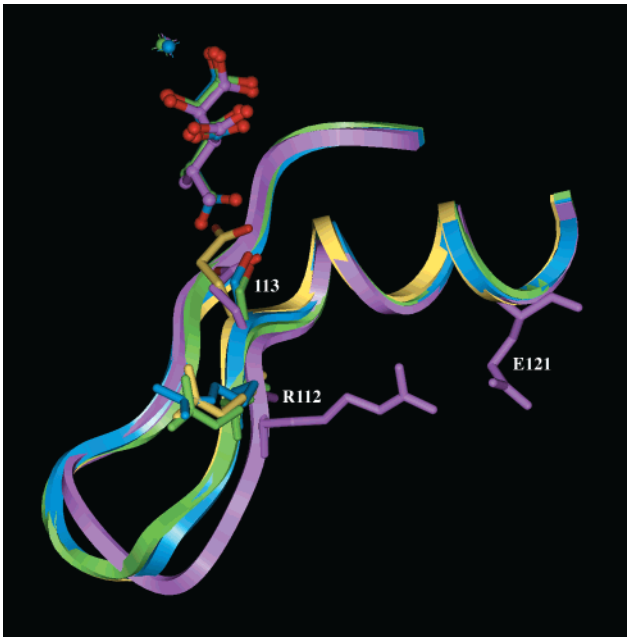

FIGURE 4: Superpositions showing the altered conformation of IPM·IDH^{S113E} loop 100−112. Enzyme and their substrates are shown as follows: IPM·IDH^{S113E} (pink), IDH^{S113E} (yellow), ISO·IDH^{Y160F} (blue), and IPM·IDH (green). Substrates and Mg^{2+} are shown in ball-and-stick rendering, and residues 112 and 113 (and residue 121 for IPM·IDH^{S113E}) are shown in stick rendering.

4 and 5). This tilt not only affects the first few residues of the helix including position 113, shifting its α carbon by 1.4 Å, but also impacts residues farther down the helix that are associated with substrate binding, such as N115 (0.7 Å) and V116 (0.8 Å).

Changes in Substrate Position. Isopropylmalate binds at the S113E active site in a position almost identical to isopropylmalate in IPM·IDH and isocitrate in ISO·IDH^{Y160F} (Figure 5). The isopropylmalate bound to IDH^{S113E} is tilted

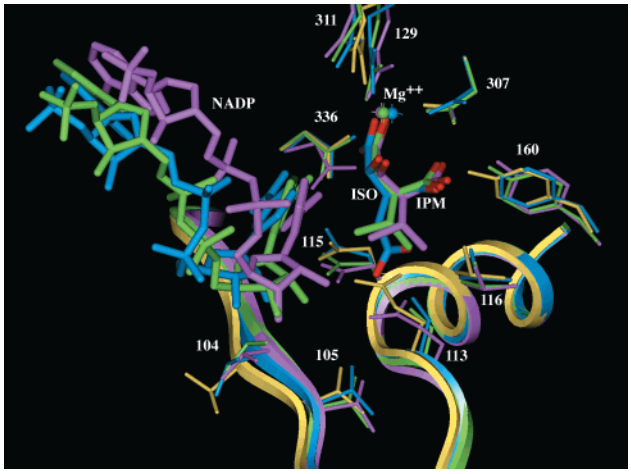

FIGURE 5: Superpositions showing the active site region. Enzymes and their substrates are shown as follows: IPM·IDH^{S113E} (pink), IDH^{S113E} (yellow), ISO·IDH^{Y160F} (blue), and IPM·IDH (green). The active site loop and helix are shown as a ribbon, and active site side chains and ligands are shown in stick rendering.

away slightly from the active site and NADP as compared to isopropylmalate bound to wild-type IDH, with C1 and C2 positions being virtually identical and C3−C7 differing by increasing distances of 0.4−0.7 Å, respectively. Isopropylmalate in the IPM·IDH^{S113E} complex is also related in a nearly identical manner to the bound isocitrate of the ISO·IDH^{Y160F} complex, with C1−C5 positions differing by increasing distances of 0.5−1.1 Å, respectively.

Larger differences are observed in the positions of NADP than for isopropylmalate and isocitrate. The X-ray data suggested a qualitative difference in the binding of NADP to these enzymes, based on the strength of the electron density (Figure 1B) and on thermal (B) factors of this substrate relative to the protein. While clear and continuous density was observed for the nicotinamide ring and adjacent ribose of NADP in IPM·IDH^{S113E}, indicating a well-ordered substrate, noncontinuous density was observed in the maps of the IPM·IDH structure (A. Mesecar and D. E. Koshland, Jr., unpublished results), suggesting a more loosely bound and less well-defined substrate. This was also reflected in a change in the apparent affinity (K_M) of NADP in the presence of isopropylmalate, from the wild-type IDH value of 77 μM to 17 μM for the S113E IDH enzyme.[2] Although this region of NADP was somewhat defined in the ISO·IDH^{Y160F} structure, atom positions are difficult to assign with accuracy due to the lower quality density maps obtained from the Laue diffraction experiments (*21*). Therefore, NADP appears better ordered in IPM·IDH^{S113E}, which may be due in part to the changes in the associated loop and helix regions of the binding site, as mentioned above.

Given these positional assignments, NADP is bound to the S113E mutant in a very different position and orientation than in the wild-type and Y160F enzymes in the presence of isopropylmalate and isocitrate, respectively (Figure 5). The adenine and phosphodiester portions of NADP, which are well defined in all three structures, clearly occupy different

[2] Previous kinetic studies of IDH have shown the K_M of isocitrate to equal the thermodynamic dissociation constant, suggesting that $1/K_M$ may be a good measure of substrate affinity (*4*). Since we are dealing with a mutant enzyme and different substrates, thermodynamic studies would need to be performed to certify this conclusion.

positions. The nicotinamide ring, however, is more similar in position and angle in each structure.

The relationship between NADP and isocitrate or isopropylmalate can be characterized by two measurements. The first is the distance between the hydride donor (C2 carbon of the malate moiety) and the hydride acceptor (C4 of the nicotinamide ring of NADP). The second is the angle defined by the nicotinamide nitrogen and C4 carbon atoms (in the plane of the ring) to the hydride donor C2 carbon of the substrate (*22*). The respective distance and angle values were 3.5 Å and 102° for IPM·IDH^{S113E}, 3.8 Å and 111° for IPM·IDH, and 3.7 Å and 129° for ISO·IDH^{Y160F}.

Local Changes. (A) E113 Position and Interactions. The position of residue 113 is altered significantly in the IPM·IDH^{S113E} structure as compared to the other three structures (Figure 5). This is probably due to the movement of the active site loop and tilt of the helix in IPM·IDH^{S113E}, in addition to the presence of NADP. In IPM·IDH^{S113E}, residue 113 is farthest from the active site, followed by IPM·IDH (C-α 1.6 Å closer), and then ISO·IDH^{Y160F} and IDH^{S113E} (both 1.8 Å closer). This causes the carboxyl group of E113 in IPM·IDH^{S113E} to be positioned very differently than E113 in the unliganded structure (a 1.4 Å shift), even though both glutamate residues adopt nearly identical conformations. E113 forms hydrogen bonds with T105 and N115. In addition, its β and γ carbons are in proximity to the isopropyl group of the substrate, which potentially stabilizes the binding of isopropylmalate through hydrophobic interactions. E113 allows a different set of interactions to be made among the substrates, cofactor, and active site residues, which has a direct impact on the binding of isopropylmalate and the catalytic performance of the enzyme.

(B) Catalytic Residue Y160. The movement of catalytic residue Y160 is one of only two structural changes identified in domain 2 that affects both the backbone and side chain (Figure 5). The position of this residue in IPM·IDH^{S113E} differs the most from IDH^{S113E}, with the C-α 1.2 Å closer to the active site, followed by ISO·IDH^{Y160F} (1.0 Å) and then IPM·IDH (0.3 Å). The hydroxyl group of Y160 in IPM·IDH^{S113E}, which points into the active site in proximity to the β-carboxyl group of the substrate, is 1.4 Å closer to the active site than in IDH^{S113E} and 0.5 Å closer than in IPM·IDH.

DISCUSSION

This report presents a crystallographic analysis of the S113E mutant of IDH, which is improved in its ability to bind isopropylmalate, an alternative substrate, and catalyze its oxidative decarboxylation. While this mutation conferred only modest improvements in kinetic constants (2−3-fold) toward substrates similar to isopropylmalate (e.g., malate, methylmalate, ethylmalate, propylmalate), it yielded significant improvements in activity toward isopropylmalate (37-fold K_M, 1.6-fold k_{cat}). This mutant has served as a starting point for additional targeted and random mutagenesis, which has further increased the kinetic constants toward isopropylmalate.

The structure of S113E in a complex with substrates displays many differences from the other structures used for comparison, which highlights changes due to the S113E mutation that are distinct from the changes caused by the components of the active complex, isopropylmalate, Mg^{2+}, and NADP. Since active sites often undergo structural changes upon substrate binding that have important consequences on catalysis by an enzyme, structures containing all of the substrates involved in a chemical reaction are invaluable to our understanding of the structural bases for enzyme specificity and catalytic activity.

Superposition of the four structures (IPM·IDH^{S113E}, IDH^{S113E}, IPM·IDH, and ISO·IDH^{Y160F}) shows that they are globally similar, except for several mobile loops and other regions that are altered either by the mutation or by the presence of substrates. Despite that these enzymes range in catalytic efficiency toward their substrates by $>10^4$, the positions of substrates are very similar. The characteristic distances and angles between isopropylmalate (or isocitrate) and NADP atoms fall within the ranges that are compatible with dehydrogenase activity (*23*). Therefore, these small differences in substrate position, while important, are not solely responsible for the differences in catalytic efficiency of the enzyme. Other structural differences, such as small changes in the position of active site residues or larger changes in the conformation or flexibility of regions associated with the active site, must also contribute to the differences in dehydrogenase activity exhibited by these enzymes.

Regions that show small differences among all four structures include the interdomain hinge region and loop 255−263, which suggests conformational flexibility in these areas. The flexibility of the hinge, which affects the relationship between the two domains of IDH, is important because it affects the size and shape of the active site, which is composed of residues from both domains. It has been suggested that the substrates bind to IDH when it is in an open conformation, which promotes reorientation of domains and closing of the active site. Upon domain closure, a hydrogen-bonding network forms between the natural substrate, isocitrate, and the enzyme, as does the optimal binding pocket for NADP (*24*). Therefore, different substrates can vary significantly in their ability to promote domain movements that produce the closed conformation of the enzyme. While small interdomain hinge differences were observed among all four structures, the differences were greatest between IPM·IDH^{S113E} and the others. The IPM·IDH^{S113E} structure shows that the relationship between the two domains is altered only in the presence of isopropylmalate and the S113E mutation, presumably acting together to improve the utilization of this substrate. The loop comprising residues 255−263 also shows conformational differences in all four structures, implying that it is flexible, which is likely to have catalytic consequences, since it is in proximity to the active site in the IDH dimer. This loop was also shown to change conformation when the product of the oxidative decarboxylation of isocitrate, α-ketoglutarate, was bound to the IDH active site, which suggests that its movement is involved in the reaction mechanism (*25*).

Effects of Substrate Binding on IDH S113E. Many differences are observed between unliganded S113E and substrate-bound structures. In IPM·IDH^{S113E}, E113 displays a nearly identical rotameric conformation as in IDH^{S113E}, although its position is shifted significantly due to the helix tilt. The tilt of the N-terminal end of the active site helix was only seen in two structures, IPM·IDH^{S113E} and IPM·IDH, indicating that this reorientation was caused by the

binding of isopropylmalate and not by the S113E substitution. This tilt allows E113 to position its β and γ carbons near the isopropyl group of the substrate, contributing to the hydrophobic pocket and potentially stabilizing the binding of isopropylmalate. The positions of other residues important for substrate binding, N115 and V116, are also altered, providing additional space in the active site for the bulky γ-isopropyl group of the new substrate. Several loop and helix movements associated with NADP binding in areas near the active site are apparent, as is a change in the relationship between the two domains of the enzyme. These movements suggest a change in conformation or flexibility of the enzyme in response to substrate binding.

Combined Effects of the S113E Substitution and Substrate Binding. The degree of the active site helix tilt that was observed in both structures with bound isopropylmalate was greater in the IPM·IDH^{S113E} structure than in IPM·IDH, suggesting that the helix reorientation was probably stabilized by the shift of loop 100−112. However, the helix movement is not caused by the loop movement, since the IPM·IDH structure, which contains a similar helix tilt, does not exhibit the altered loop structure. The helix tilt in both structures similarly affects the positions of residues 115 and 116, which form the binding site for isopropylmalate and NADP. Valine 116, which contributes to the hydrophobic binding pocket for the isopropyl group of isopropylmalate, is shifted away from the active site in both structures, providing more space for the bulky isopropyl group of isopropylmalate. The improved affinity of the IDH^{S113E} enzyme for isopropylmalate, therefore, must arise from the new interactions of E113 with the other active site residues such as N115, isopropylmalate, and NADP.

(A) The Role of E113. In the IPMDH enzyme, which catalyzes the analogous reaction to IDH using isopropylmalate as its preferred substrate, a conserved active site glutamate residue resides in a location similar to S113 in IDH. This glutamate has been implicated as a major determinant of the broad substrate specificity of IPMDH, based on the position it was hypothesized to adopt in response to the binding of different substrates (*26*). The γ-carboxyl group of the glutamate was proposed to interact with one of the hydroxyl groups of the nicotinamide ribose of NAD when isopropylmalate is bound, stabilizing the substrate−cofactor complex (*26*, *27*). Comparison of IPMDH and IDH suggests that the S113E substitution in IDH could function in the same role as the corresponding glutamate of IPMDH, by forming similar interactions with the substrates. Although the structure of the IDH^{S113E} enzyme has been determined in the absence of substrates (*20*), it does not provide an explanation for the unexpected catalytic enhancement of IDH^{S113E} toward isopropylmalate. Our structure of IPM·IDH^{S113} argues against the possibility that S113E improves activity toward isopropylmalate by interacting with a ribose hydroxyl group attached to the nicotinamide ring of NADP, since the E113 carboxyl group is 4.5 Å from the closest nicotinamide ribose hydroxyl group. Residue T104, however, might provide this function, based on its proximity to the ribose moiety.

A new role for the S113E substitution is identified by the IPM·IDH^{S113E} structure on the basis of its interactions with both the isopropylmalate substrate and neighboring active site residues. Instead of interacting with the nicotinamide ribose as hypothesized, E113 forms a hydrogen bond with the T105 and the oxygen of the N115 side chain, which orients E113 for optimal van der Waals interactions with isopropylmalate. Perhaps these interactions cause a reorientation of loop residues 100−112, which is only observed in IPM·IDH^{S113E} (and not in either IDH^{S113E} or IPM·IDH), indicating that the movement is due to the combination of the S113E mutation and the presence of isopropylmalate and NADP. In the IPMDH enzyme, which catalyzes a reaction analogous to IDH using isopropylmalate as a substrate, the corresponding loop is six residues longer, contains a different amino acid sequence, and adopts a different conformation. The loop movement seen in IPM·IDH^{S113E} is very similar to that described for IPMDH, in which a "loop-closing mechanism" is thought to stabilize and align the substrates and cofactor by moving up toward the active site to aid in catalysis (*28*).

(B) Effects on NADP Binding. These new interactions among S113E, its surrounding residues, and isopropylmalate must play a role in changing the binding site of NADP, since IPM·IDH is structurally different. In addition to the altered conformation of bound NADP in the IPM·IDH^{S113E} structure, the well-defined nicotinamide group of NADP suggests significant differences in its mode of binding. A number of structural changes appear to operate together to accommodate NADP. Global reorientation of the two domains may improve the NADP-binding site by reducing the volume of the active site cleft. The interaction of E113 with N115 places the N115 side chain nitrogen 3.0 Å from the carboxyamide oxygen of NADP. This interaction, combined with the interaction of E336 with the carboxyamide nitrogen in the IPM·IDH^{S113E} structure, may stabilize binding of the nicotinamide ring. The NADP binding loop (336−355) and helix (390−396) regions move in toward the active site to alter the binding site of NADP, which may be related to the movement of E336, which shifts its position in relation to the other structures and interacts with the carboxyamide group of the nicotinamide ring. The loop (100−112) that connects the NADP binding area to the active site helix also moves in toward the substrates, possibly stabilizing their orientations as well.

(C) The Role of N115. These new interactions lead to a newly proposed role for N115 as well. When the natural substrate, isocitrate, is bound to the enzyme, N115 is thought to form an electrostatic interaction with the γ-carboxylate of isocitrate (*6*) and also to contact the C4 carbon of the nicotinamide ring of NADP to promote catalysis (*3*). In this role, N115 is thought to be nonessential, however, since substitution of this residue only reduces the k_{cat} 50-fold (*29*). When isopropylmalate is the substrate, the structural rearrangements and interactions that alter the position and interactions of N115 make it an integral residue in both binding and catalysis. This explains why random mutagenesis experiments of several active site residues, including N115, aiming to identify enzymes with improved activity toward isopropylmalate, resulted mostly in mutants that were unchanged in this position (*8*). Site-directed mutants containing the N115 to leucine substitution (based on the IPMDH sequence), which were created to change the substrate specificity to isopropylmalate, displayed no detectable activity toward isopropylmalate, whereas otherwise similar mutants containing the wild-type residue N115 were enhanced in their level of activity (*8*).

(D) Substrate Affinity and Catalysis. While the S113E enzyme binds its new substrate isopropylmalate as well as the native enzyme binds isocitrate, barriers still exist that prevent a significant improvement in catalytic rate. It is difficult to relate the observed changes in structure to the minimal improvement in k_{cat}. One reason for this difficulty is the absence of knowledge on the structural changes that the enzyme undergoes during catalysis, even when detailed pictures of the free enzyme and the enzyme−substrate complex are available. Despite these limitations, unique structural changes that affected secondary structural elements in the active site as well as the relationship of domains of IDH were identified that are specific to the binding of alternative substrates.

CONCLUSION

Analysis of the structure of the IPM·IDH^{S113E} active complex and its comparison to similar wild-type and mutant structures with various substrates have elucidated how the S113E mutation confers improved specificity for isopropylmalate. The binding of the new substrate, isopropylmalate, and NADP triggers conformational changes that affect the interactions of enzyme and substrate. E113 interacts with isopropylmalate directly and with NADP indirectly through N115, which together lead to significantly improved binding of isopropylmalate and a modest improvement in the catalytic rate. Many other structural changes were observed, including an altered conformation of several loops and a change in the angle of the hinge between domains 1 and 2. These global and local changes in protein conformation and flexibility evidently play an important role in changing the substrate specificity of IDH, which exemplifies some of the many ways proteins can be altered to change their function.

ACKNOWLEDGMENT

X-ray diffraction data were collected at the Advanced Light Source (ALS), beam line 5.0.2, Lawrence Berkeley National Laboratory (LBNL). ALS is supported by the Director, Office of Science, Office of Basic Energy Sciences, Materials Sciences Division, of the U.S. Department of Energy under Contract DE-AC03-76SF00098 at Lawrence Berkeley National Laboratory. This work was in part carried out under the auspices, also, of Contract W7405-ENG-4H.

REFERENCES

1. Stemmer, W. P. C. (1994) *Nature 370*, 389−391.
2. Yano, T., Oue, S., and Kagamiyama, H. (1998) *Proc. Natl. Acad. Sci. U.S.A. 95*, 5511−5515.
3. Bolduc, J. M., Dyer, D. H., Scott, W. G., Singer, P., Sweet, R. M., Koshland, D. E., Jr., and Stoddard, B. L. (1995) *Science 270*, 365−365.
4. Dean, A. M., and Koshland, D. E., Jr. (1993) *Biochemistry 32*, 9302−9309.
5. Dean, A. M., Shiau, A. K., and Koshland, D. E., Jr. (1996) *Protein Sci. 5*, 341−347.
6. Hurley, J. H., Dean, A. M., Koshland, D. E., Jr., and Stroud, R. M. (1991) *Biochemistry 30*, 8671−8678.
7. Lee, M. E., Dyer, D. H., Klein, O. D., Bolduc, J. M., Stoddard, B. L., and Koshland, D. E., Jr. (1995) *Biochemistry 34*, 378−384.
8. Doyle, S. A., Fung, S. F., and Koshland, D. E., Jr. (2000) *Biochemsitry* (in press).
9. Mesecar, A. D., and Koshland, D. E., Jr. (2000) *IUBMB Life 49*, 457−466.
10. Dean, A. M., Lee, M. H. I., and Koshland, D. E., Jr. (1989) *J. Biol. Chem. 264*, 20482−20486.
11. Leslie, A. G. W. (1992) *CPCr and ESF-EACMB Newsletter on Protein Crystallography 26*.
12. CCP4 (1994) *Acta Crystallogr. D50*, 760−763.
13. Brunger, A. T. (1992) *Acta Crystallogr. D*, 24−36.
14. Jones, T. A., Zou, J. Y., Cowan, S. W., and Kjeldgaard, M. (1991) *Acta Crystallogr. A47*, 110−119.
15. Lamzin, V. S., and Wilson, K. S. (1997) *Methods Enzymol. 277*, 269−305.
16. Hooft, R. W. W., Vriend, G., Sander, C., and Abola, E. E. (1996) *Nature 381*, 272−272.
17. Fauman, E. B., Rutenber, E. E., Maley, F., and Stroud, R. M. (1994) *Biochemistry 33*, 1502−1511.
18. McRee, D. E. (1992) *J. Mol. Graphics 10*, 44−47.
19. Merritt, E. A., and Bacon, D. J. (1997) *Methods Enzymol. 277*, 505−524.
20. Hurley, J. H., Dean, A. M., Sohl, J. L., Koshland, D. E. and Stroud, R. M. (1990) *Science 249*, 1012−1016.
21. Stoddard, B. L., Dean, A., and Bash, P. A. (1996) *Nat. Struct. Biol. 3*, 590−595.
22. Mesecar, A. D., Stoddard, B. L., and Koshland, D. E., Jr. (1997) *Science 277*, 202−206.
23. Stoddard, B. L., Dean, A., and Koshland, D. E., Jr. (1993) *Biochemistry 32*, 9310−9316.
24. FinerMoore, J., Tsutakawa, S. E., Cherbavaz, D. B., LaPorte, D. C., Koshland, D. E., Jr., and Stroud, R. M. (1997) *Biochemistry 36*, 13890−13896.
25. Stoddard, B. L., and Koshland, D. E., Jr. (1993) *Biochemistry 32*, 9317−9322.
26. Imada, K., Inagaki, K., Matsunami, H., Kawaguchi, H., Tanaka, H., Tanaka, N., and Namba, K. (1998) *Structure 6*, 971−982.
27. Dean, A. M., and Dvorak, L. (1995) *Protein Sci. 4*, 2156−2167.
28. Hurley, J. H., and Dean, A. M. (1994) *Structure 2*, 1007−1016.
29. Chen, R. D., Grobler, J. A., Hurley, J. H., and Dean, A. M. (1996) *Protein Sci. 5*, 287−295.
30. Wallon, G., Yamamoto, K., Kirino, H., Yamagishi, A., Levett, S. T., Petsko, G. A., and Oshima, T. (1997) *Biochim. Biophys. Acta 1337*, 105−112.
31. Read, R. J. (1986) *Acta Crystallogr. A42*, 140−149.

BI002533Q